Harmonic analysis on the Lorentz group and the hadron–hadron elastic-scattering amplitude

S. B. Drenska and S. Sh. Mavrodiev

Joint Institute for Nuclear Research, Dubna

Fiz. Elem. Chastits At. Yadra **15**, 94–120 (January–February 1984)

The amplitude of elastic proton–proton scattering at high energies is constructed on the basis of simple quantum-mechanical assumptions and a relativistic relative-coordinate space. Descriptions of $(d\sigma/dt)(s,t)$, $\sigma_t(s)$, and $\rho(s)$ are obtained. The amplitude depends on the energy through a function $R(s)$, which in accordance with the optical theorem determines the total cross section by the formula $\sigma_t(s) = 2\pi R^2(s)$ and can be interpreted as the effective range of the hadron–hadron interaction. The dependence of the hadron–hadron total cross sections on the quantum numbers of the colliding particles is investigated. Descriptions are obtained for the total $\bar{p}p$, pp, $\pi^{\mp}p$, and $K^{\mp}p$ interactions and their asymptotic behavior as $s\to\infty$.

INTRODUCTION

Study of hadron–hadron interactions at high energies is one of the topical problems of elementary-particle physics. While the relativistic mechanics of a single particle arose almost at the same time as the creation of the special theory of relativity, a relativistic theory of two interacting particles still does not exist.

In the absence of a consistent theory of strong interactions, it is natural to augment general theoretical ideas with attempts to solve preliminary problems of the heuristic systematics of elementary particles[1] and experimental data on their interactions.

One of the most important methods for investigating strong-interaction dynamics is the quasipotential approach proposed and developed by Logunov and Tavkhelidze.[2] This approach and its modifications[3] have served as the basis for a number of models of the strong interaction of elementary particles (see Ref. 4 and the literature quoted there) created to describe the rich experimental material accumulated during the last 15 years with the Serpukhov, CERN ISR, and Fermilab accelerators.[5–9] There also exist a number of other models of hadron–hadron interactions at high energies,[10–15] based on the use of optical analogies in strong-interaction physics and on assumptions about the analytic properties of the scattering amplitude and the composite structure of hadrons.

Our analysis of hadron–hadron interactions at high energies is based on the following two hypotheses:

a) the strong interaction of two particles can be described by analogy with the quantum-mechanical problem of an effective particle in an effective field, and the effective field (quasipotential) depends in general on the energy[2];

b) the space of the dynamical variables (the relative momentum and relative coordinate) is not Euclidean, but rather the radius of curvature of the relative-momentum space can depend on the energy and masses of the two interacting particles.

In Sec. 1, we make the main assumptions and formulate the problem. In Sec. 2, we give the basic formulas of the relativistic Fourier analysis which relates conjugate dynamical variables.

In Sec. 3, we formulate a mathematical model of the amplitude in the space of the relativistic relative coordinate and we solve the inverse problem of finding from experimental data the number, magnitude, and statistical uncertainty of the unknown parameters. We obtain analytic expressions for the amplitude in the spaces of the relative coordinate and relative momentum. We compare the expressions obtained for $(d\sigma/dt)(s,t)$, $\sigma_t(s)$, and $\rho(s)$ with experimental data. We make a prediction about the behavior of the elastic pp cross section for the kinematically admissible momenta at higher energies.

In Sec. 4, we investigate the dependence of the total cross sections of hadron–hadron interactions on the quantum numbers of the colliding particles at energies $\sqrt{s}\geqslant 10$ GeV. We predict the behavior of the total proton–hyperon cross sections and also of some proton–nucleus interactions at high energies. We investigate the behavior with increasing energy of some quark sum rules.

In Sec. 5, we obtain a phenomenological description of the total $\bar{p}p$, pp, $\pi^{\mp}p$, and $K^{\mp}p$ interaction cross sections from the threshold energies in terms of the effective interaction range. We investigate the asymptotic behavior of the expressions obtained for the total cross sections of particles and antiparticles.

In Sec. 6, we give the main results and predictions.

To solve overdetermined systems of nonlinear algebraic equations we use a method of self-regularized iterative processes of the Gauss–Newton type.[16]

To obtain graphical information, we used the language SIGMA[17] and the program package HPLOT.[18]

1. ASSUMPTIONS AND FORMULATION OF THE PROBLEM

To study a two-particle relativistic system in the framework of the Feynman–Dyson four-fermion formalism, one can use the completely covariant Bethe–Salpeter equation.[19] Despite its advantages, in this approach there is no clear physical understanding of the dependence of the wave function on the relative time of the two particles.

By virtue of its probabilistic interpretation of the wave function for the two-particle problem, the quasipotential approach makes it possible to use physically perspicuous quan-

 0090-4759/84/010042-12$04.40

tum-mechanical analogies. In its ideas, the quasipotential approach is close to the optical model of the nucleus, the scattering problem being regarded, not as a two-particle problem, but as the motion of a nucleon in a field described by a quasipotential. In the case of strong interactions, a regular method for constructing the quasipotential does not exist. Usually, it is constructed phenomenologically on the basis of general principles,[11] a Gaussian potential being taken as a first approximation.

The ambiguity associated with the continuation of the amplitude off the mass shell leads to the problem of determining the mass of the effective particle.[20]

In nonrelativistic quantum mechanics (see, for example, Ref. 21), in which we have the Schrödinger equation and the method of introducing the interaction is known, the two-body problem reduces to the problem of one effective particle in an effective field. A unit representation of the Galileo group (see Ref. 22 and the references given there) is realized (up to rotation) on the space of the effective wave function. The translation group of the relative-momentum space is isomorphic to the group of Galilean boosts but is not a covariance group of the equation. Reduction of the unitary representations of this group to irreducible representations leads to harmonic analysis[23] with a three-dimensional exponential. This Fourier analysis relates the nonrelativistic relative coordinate to the nonrelativistic relative momentum. The group-theoretical analysis of the nonrelativistic hydrogen atom shows that the three-dimensional plane wave of the free motion of the effective particle is not the three-dimensional part of the four-dimensional plane wave $\exp[i(Et - \mathbf{p}\cdot\mathbf{x})]$ of the center-of-mass motion but appears on the decomposition into irreducible representations of the regular representation of the group of shifts of the relative-momentum space,[24] i.e., if the geometry of the relative-momentum space of the two-particle system is known, then, following the above-mentioned group-theoretical construction, one can determine the relative-coordinate space of the system.[24]

The integral representation of the elastic-scattering amplitude in the form of the Fourier expansion

$$T(\mathbf{q}) = -\frac{m}{4\pi}\int d^3\mathbf{r}\exp(-i\mathbf{q}\cdot\mathbf{r})\,T(\mathbf{r}), \qquad (1)$$

where $\mathbf{q}$ is the momentum transfer, can be interpreted as the Born approximation for the solution of the Schrödinger equation, and in the case of the Coulomb potential leads to Rutherford's well-known expression (see, for example, Ref. 21).

In the papers of Ref. 3, which are based on the Hamiltonian formulation of quantum field theory, a variant of the quasipotential approach to the relativistic two-particle problem is developed in which three-dimensionality plays an integral part from the very beginning. All virtual particles are on their mass shells. By virtue of the three-dimensionality, one can construct in this approach equations describing two-particle relativistic systems that have the same form as the corresponding nonrelativistic Schrödinger and Lippmann–Schwinger equations. In contrast to the nonrelativistic equations, all integrations in this case are over a three-dimensional Lobachevskii momentum space. This space is realized on the upper sheet of the hyperboloid

$$q = (\sqrt{m^2 + \mathbf{q}^2},\ \mathbf{q}), \qquad (2)$$

i.e., on the mass shell of one relativistic particle. The group of motions of Lobachevskii space is the Lorentz group. The decomposition into irreducible representations of the regular representation of the Lorentz group on the space of functions that are square-integrable on the hyperboloid (2) [1)] leads to relativistic Fourier analysis.[24] A connection appears between the space of the three-dimensional relative momentum $\mathbf{q}$ of the two-particle system and the space of the three-dimensional relative coordinate $\mathbf{r}$.

In the present paper, following the formulation of the quasipotential approach in Ref. 3 and the idea of geometrization of the relativistic two-body problem,[26] we assume that the relative momentum of the effective particle of a two-hadron relativistic system belongs to the Lobachevskii space (2), and that the effective mass may depend both on the masses m_1 and m_2 of the colliding particles and on the energy[2)] $s = (p_1 + p_2)^2$, i.e., $m = m(m_1, m_2, s)$. The relativistic analog of (1) is the integral representation

$$T(s,\ t) = -\frac{m}{4\pi}\int d^3\mathbf{r}\,\overset{+}{\xi}(m,\ \mathbf{q},\ \mathbf{r})\,T(s,\ \mathbf{r}), \qquad (3)$$

where $t = (p_1 - p_3)^2 + \ - \mathbf{q}^2$ is the square of the momentum transfer, and in the spinless case

$$\xi(m,\ \mathbf{q},\ \mathbf{r}) = \left(\frac{\sqrt{m^2+\mathbf{q}^2} - \mathbf{q}\cdot\mathbf{n}}{m}\right)^{-1-imr},\quad \mathbf{n}^2 = 1,$$

where $\mathbf{t}$ is interpreted as a relative momentum, and $\mathbf{r} = r\mathbf{n}$ as a relative coordinate. Because a relativistic plane wave goes over when $|\mathbf{q}| \ll m$ into the ordinary three-dimensional exponential $\exp(-i\mathbf{q}\cdot\mathbf{r})$, power-law behavior of $T(s,t)$ at large momentum transfers $|t|$ goes over into exponential behavior for $\sqrt{|t|} \ll m$, i.e., Eq. (3) makes it possible to describe qualitatively the experimentally observed exponential–power-law behavior of the elastic differential cross section. On the basis of this property of the integral representation (3), we investigate the possibility of constructing an elastic pp scattering amplitude[28] that describes quantitatively all the experimental data on $(d\sigma/dt)(s,t)$, $\sigma_t(s)$, and $\rho(s)$ for $\sqrt{s} \geqslant 10$ GeV and $0.0375 \leqslant |t| \leqslant 9.75$ GeV^2.[3)]

2. RELATIVISTIC FOURIER ANALYSIS

In nonrelativistic quantum mechanics, analysis of a two-particle stationary system shows that information about the dynamics of the system is contained in the wave function of the relative momentum (or coordinate) of the two particles. A unit representation of the Galileo group[22] is realized (up to rotation) on the space of the effective wave function. Reduction of the unitary representations of the translation group of the relative-momentum space into irreducible representations leads to three-dimensional harmonic analysis with the three-dimensional exponential $\exp(-i\mathbf{q}\cdot\mathbf{r})$. The ba-

[1)] In Ref. 25, these representations of the Lorentz group were used for the first time to expand a scattering amplitude.

[2)] In Ref. 27, for example, the effective mass is given by the expression $m_{\text{eff}} = \sqrt{m_1^2 + \mathbf{q}^2} + \sqrt{m_2^2 + \mathbf{q}^2}/\sqrt{s}$, where $\mathbf{q}$ is the c.m.s. relative momentum.

[3)] In this paper, we assme $\hbar = c = 1$.

sic formula of nonrelativistic analysis, which connects the momentum and coordinate representations, has, as is well known, the form

$$\Psi(\mathbf{q}) = \frac{1}{(2\pi)^{3/2}} \int d^3\mathbf{r} e^{-i\mathbf{q}\cdot\mathbf{r}} \Psi(\mathbf{r}). \quad (4)$$

If a representation of the group T_q of Galilean boosts is given in the momentum space, i.e.,

$$T_q \Psi(\mathbf{p}) = \Psi(\mathbf{p} - \mathbf{q}),$$

then T_q can be decomposed into irreducible representations $T_q^{[r]}$, which act on the coordinate space as follows:

$$T_q^{[r]} \Psi(\mathbf{r}) = e^{-\mathbf{q}\cdot\mathbf{r}} \Psi(\mathbf{r}).$$

As is well known, the Heisenberg uncertainty relation

$$\Delta r \, \Delta p \geqslant \hbar/2,$$

can be obtained as a consequence of (4) and the diagonality of the coordinate and momentum operators in the p and r representations, respectively.

Let $\psi_\mu^{(S)}(\mathbf{q})$ be the relativistic wave function of the effective particle of a system of two hadrons with mass m, spin S, spin projection μ, and momentum $\mathbf{q}$, this last belonging to a Lobachevskii space.

A representation of the Lorentz group is given by[4)]

$$T_p \Psi_\mu^{(S)}(\mathbf{q}) = \sum_{\mu'=-S}^{S} D_{\mu\mu'}^{(S)}(V(p, q)) \Psi_{\mu'}^{(S)}(\mathbf{q}(-)\mathbf{p}),$$

where

$$q(-)p = \Lambda_p^{-1} q = \begin{pmatrix} \frac{q_0 p_0 - \mathbf{q}\cdot\mathbf{p}}{m_p} \\ \mathbf{q} - \frac{\mathbf{p}}{m_p} \frac{m_p q_0 + q_0 p_0 - \mathbf{q}\cdot\mathbf{p}}{m_p + p_0} \end{pmatrix}$$

$$\equiv \begin{pmatrix} \frac{qp}{m_p} \\ \mathbf{q} - \frac{\mathbf{p}}{m_p} \frac{m_p q_0 + qp}{m_p + p_0} \end{pmatrix},$$

$$q_0 = \sqrt{m_q^2 + \mathbf{q}^2}, \quad p_0 = \sqrt{m_p^2 + \mathbf{p}^2}.$$

The matrix of a Wigner rotation V has the form

$$V(p, q) = B_q^{-1} B_p B_{q(-)p} = V^{-1}(q, p),$$

where

$$B_p = \frac{m_p + p}{\sqrt{2m_p(m_p + p_0)}},$$

and

$$p = p^\mu \sigma_\mu = p_0\sigma_0 - \mathbf{p}\cdot\boldsymbol{\sigma} = \begin{pmatrix} p^0 + p^3 & p^1 - ip^2 \\ p^1 + ip^2 & p^0 - p^3 \end{pmatrix}.$$

The Pauli matrices are

$$\sigma = \left[\begin{pmatrix} 1 & 0 \\ 0 & 1 \end{pmatrix}, \begin{pmatrix} 0 & 1 \\ 1 & 0 \end{pmatrix}, \begin{pmatrix} 0 & -i \\ i & 0 \end{pmatrix}, \begin{pmatrix} 1 & 0 \\ 0 & -1 \end{pmatrix} \right].$$

The matrix elements of the rotation representation of weight S have the form

$$D_{\mu\nu}^{(S)}(\mathbf{n}) = \left(\frac{(S+\nu)!\,(S-\nu)!}{(S+\mu)!\,(S-\mu)!} \right)^{1/2} \exp[i(-\mu+\nu)\varphi]$$

$$\times \sum_k (-1)^{S-\nu+k} \binom{S-\mu}{k} \binom{S+\mu}{S-\nu-k}$$

$$\left(\cos\frac{\theta}{2}\right)^{\mu+\nu+2k} (\sin\theta/2)^{2S-\mu-\nu-2k},$$

$$\mathbf{n} = \begin{pmatrix} \sin\theta\cos\varphi \\ \sin\theta\sin\varphi \\ \cos\theta \end{pmatrix}, \quad n^2 = 1.$$

The decomposition of the representation T_p of the Lorentz group into irreducible representations $T_p^{[\nu,r]}$ for $\nu = -S, \ldots, S$, $0 \leqslant r \leqslant \infty$ is given by

$$\left.\begin{aligned} \Psi_\mu^{(S)}(\mathbf{q}) &= \frac{1}{(2\pi)^{3/2}} \sum_{\nu=-S}^{S} \int_0^\infty (\nu^2 + r^2)\, dr \int d^2\mathbf{r}\, \overset{+}{\xi}{}_{\mu\nu}^{(S)}(m, \mathbf{q}, \mathbf{r})\, \Psi_\nu^{(S)}(\mathbf{r}), \\ \Psi_\mu^{(S)}(\mathbf{r}) &= \frac{1}{(2\pi)^{3/2}} \sum_{\nu=-S}^{S} \int \frac{d^3\mathbf{q}}{2\sqrt{m^2 + \mathbf{q}^2}} \xi_{\mu\nu}^{(S)}(m, \mathbf{q}, \mathbf{r})\, \Psi_\nu^{(S)}(\mathbf{q}), \end{aligned}\right\} \quad (5)$$

where $d^2\mathbf{r} = \sin\theta\cos\theta\, d\varphi$.

The relativistic plane wave is

$$\xi_{\mu\nu}^{(S)}(m, \mathbf{q}, \mathbf{r}) = \xi(m, \mathbf{q}, \mathbf{r})\, D_{\mu\nu}^{(S)}(\mathbf{r}(-)\mathbf{p}),$$

where

$$\xi(m, \mathbf{q}, \mathbf{r}) = \left(\frac{\sqrt{m^2 + \mathbf{q}^2} - \mathbf{q}\cdot\mathbf{n}}{m} \right)^{-1 - imr}, \; S = 0. \quad (6)$$

The analog of the Heisenberg uncertainty relation in the case of zero spin and the Fourier analysis (5) will be the following relation[5)] between the rapidity and the relativistic coordinate[24]:

$$\Delta\chi \Delta r \geqslant \frac{\hbar}{2mc}.$$

The dynamical Feynman variable—the rapidity—is given by

$$\chi = \ln\left(\sqrt{1 + \frac{\mathbf{q}^2}{m^2}} + \frac{|\mathbf{q}|}{m} \right). \quad (7)$$

In spherical coordinates, the momentum of the effective particle can be expressed in terms of the rapidity by

$$q = \begin{pmatrix} m \operatorname{ch}\chi \\ m \operatorname{sh}\chi \mathbf{n} \end{pmatrix}, \quad \mathbf{n}^2 = 1.$$

In accordance with (6) and (7), we can show that

$$\lim_{|\mathbf{q}| \ll m} \xi(m, \mathbf{q}, \mathbf{r}) = \exp(i\mathbf{q}\cdot\mathbf{r}); \quad (8)$$

$$\lim_{|\mathbf{q}| \ll m} \chi = \frac{|\mathbf{q}|}{m}. \quad (9)$$

Under the integral sign the composition theorem for relativistic plane waves holds:

$$\int d^2\mathbf{r}\, \overset{+}{\xi}{}^{(S)}(m, \mathbf{q}, \mathbf{r})\, \xi^{(S)}(m, \mathbf{p}, \mathbf{r})$$

$$= D^{(S)}(V(p, q)) \int d^2\mathbf{r}\, \overset{+}{\xi}{}^{(S)}(m, \mathbf{q}(-)\mathbf{p}, \mathbf{r})\, D^{(S)}(\mathbf{r}).$$

It is well known that in nonrelativistic quantum mechanics the Born amplitude is the three-dimensional Fourier transform of the interaction potential. In the relativistic case, we know neither the exact equation (together with the boundary conditions) nor the quasipotential. We therefore assume that the elastic hadron–hadron scattering amplitude has the integral representation[6)]

$$T(s, t) = -\frac{m}{4\pi} \int d^3\mathbf{r}\, \overset{+}{\xi}(m, \mathbf{t}, \mathbf{r})\, T(s, \mathbf{r}). \quad (10)$$

[4)]Here, we use the notation of Ref. 29.

[5)]For clarity, we have here restored the dimensional constants.

[6)]For simplicity, we here take spin $S = 0$.

Then, by virtue of the property (8) of the relativistic plane wave $\xi(m,\mathbf{t},\mathbf{r})$, behavior of the amplitude $T(s,\mathbf{r})$ in the relative coordinate space such that $T(s,t)$ has the power-law behavior $\sim t^{-a}$ means that for $\sqrt{|t|} \ll m$ this behavior goes over into the exponential $\sim e^{-at}$. Thus, the exponential–power-law behavior of the elastic differential cross section can be explained by the fact that the local geometry on the hyperboloid is Euclidean geometry. This assertion can be readily understood on the basis of a mnemonic: The formulas of nonrelativistic Fourier analysis go over into the relativistic ones by means of the substitution

$$\sqrt{-t} \to m\chi = m \ln\left(\sqrt{-\frac{t}{m^2}} + \sqrt{1-\frac{t}{m^2}}\right),$$

i.e.,

$$\exp(-bm\chi) = \left(\sqrt{-\frac{t}{m^2}} + \sqrt{1-\frac{t}{m^2}}\right)^{-bm} \xrightarrow[\sqrt{-t} \ll m]{} \exp\left(-b\sqrt{-t}\right).$$

3. AMPLITUDE OF ELASTIC *pp* SCATTERING

We assume that the integral representation (10) holds for the elastic *pp* scattering amplitude. We represent the amplitude $T(s,r)$ in the r space in the form

$$T(s,\ r,\ A) = \sum_k \frac{a_k(s)\, e^{-b_k(s)r}}{c_k(s) - r + id_k(s)}, \tag{11}$$

where a_k, b_k, c_k, d_k are unknown functions of the energy, and A is a set of unknown parameters. This choice of $T(s,r)$ is dictated by the analogy with the quantum mechanics of a many-electron atom and the exponential–power-law behavior of elastic *pp* scattering. We note that in the framework of quantum field theory a similar behavior in r space was obtained for the so-called singular potentials (see Ref. 30).

The expression (10) in the case of the spherical potential (11) takes the form

$$T(s,\ t,\ A) = -\frac{1}{\sinh\chi}\int_0^\infty dr\, r \sin(m\chi r)\, T(s,\ r,\ A), \tag{12}$$

where

$$\chi = \ln\left(\sqrt{-\frac{t}{m^2}} + \sqrt{1-\frac{t}{m^2}}\right).$$

Requiring also that the elastic amplitude satisfy the condition of crossing symmetry, we make the substitution

$$T \to T(s,\ t,\ A) + T(s,\ u,\ A),$$

where

$$s + t + u = 4m^2.$$

To determine the number, magnitude, and statistical uncertainty of the parameters A, we must compare the mathematical model (12) with experimental data.[5–9] This leads to the following overdetermined system of nonlinear algebraic equations:

$$\frac{d\sigma^{\exp}}{dt}(s,\ t) = \frac{|T(s,\ t,\ A)|^2}{16\pi s(s-s_0)};$$

$$\sigma_t^{\exp}(s) = \frac{\operatorname{Im} T(s,\ 0,\ A)}{\sqrt{s(s-s_0)}};$$

$$\rho^{\exp}(s) = \frac{\operatorname{Re} T(s,\ 0,\ A)}{\operatorname{Im} T(s,\ 0,\ A)},$$

TABLE I. Energies, momentum transfers, the number of measured points, and the values of χ^2_S, χ^2_{SN}, and χ^2.

s, GeV^2	$\lvert -t_{\min}\rvert$, GeV^2	$\lvert -t_{\max}\rvert$, GeV^2	Number of points	χ^2_S	χ^2_{SN}	χ^2
95.607	0.0375	0.75	18	165.997	157.456	24.033
133.135	0.0375	0.70	19	233.193	189.912	20.208
189.429	0.0375	0.70	20	70.688	58.659	5.598
264.491	0.0375	0.80	21	180.418	169.085	19.795
330.171	0.0375	0.70	17	575.472	282.552	19.146
547.56	0.825	5.75	57	140.359	134.560	57.184
930.25	0.875	5.75	56	179.301	144.760	103.923
1989.160	0.875	7.25	59	118.737	117.316	50.961
2737.840	0.825	9.75	65	114.552	91.705	45.218
3856.410	0.825	6.25	58	96.387	60.492	54.864

where $s_0 = 4m_p^2$. This system can be solved by a method of self-regularized iterative processes of Gauss–Newton type.[16] One minimizes the expression

$$\chi^2 = \sum^{M} \left(\frac{y^{\exp} - y^{\text{theor}}}{\Delta}\right)^2,$$

where $y^{\exp}$ and y^{theor} are the left- and right-hand sides of the equations, respectively, and M is the number of all the equations. The solution of the system has been investigated in the following cases:

1. $\Delta = \Delta^{\text{stat}}(\chi^2_S)$;
2. $\Delta = \Delta^{\text{stat}}(\chi^2_{SN})$, but in this case an additional attempt was made at more accurate determination of the normalizations of the differential cross sections, i.e., the number of parameters was increased by the number of different energies;
3. $\Delta = \Delta^{\text{stat}} + \Delta^{\text{syst}}(\chi^2)$.

In the cases when expressions of the type (12) cannot be integrated analytically, we use the fast integration programs SFUSIN and SFUCOS.[31]

In Table I, we give the energies, momentum transfers, number of measured points, and values of χ^2_S, χ^2_{SN}, and χ^2 for the determined parameters A in the solution of the overdetermined system

$$\chi^2_S/(M-N) = \frac{1875}{390-23} = 5.11;$$

$$\chi^2_{SN}/(M-N) = \frac{1407}{390-33} = 3.94;$$

$$\chi^2/(M-N) = \frac{401}{390-23} = 1.09;$$

$$\chi^2_S/(M-N)_{\substack{\text{CERN}\\\text{DATA}}} = 2.39, \quad \chi^2_{SN}/(M-N)_{\substack{\text{CERN}\\\text{DATA}}} = 2.10;$$

$$\chi^2/(M-N)_{\substack{\text{CERN}\\\text{DATA}}} = 1.15,$$

where N is the number of unknown parameters.

For our solution, the mass of the effective particle and the amplitude have the form

$$m(s) = a_1 R(s), \tag{13}$$

$$R(s) = a_2 + a_3/(s/s01)^{a_4} + a_5 \ln(s/s01), \tag{14}$$

where[7)]

$$s01 = (1.81 \pm 0.06)\text{GeV}^2; \tag{15}$$

[7)]For the determination of the scale parameter $s01$, see Sec. 4.

TABLE II. Values of the parameters A_i $(i = 1,...,23)$ and their statistical uncertainties ΔA_i.

N	A	ΔA	N	A	ΔA
1	0,18531	0,00008	13	3,465	0,002
2	0,913	0,009	14	−912,50	0,02
3	2,858	0,006	15	−8730,92	0,002
4	0,324	0,003	16	−3,290	0,002
5	0,1994	0,0008	17	82,170	0,007
6	12,4489	0,0066	18	445,54	0,02
7	7,8602	0,0003	19	0,4073	0,0009
8	8,2110	0,0005	20	−425,440	0,006
9	15,5527	0,0004	21	−224,500	0,02
10	7,1927	0,0005	22	1,402	0,002
11	15,4652	0,0003	23	465,114	0,006
12	94,3	0,1			

$$T(s,\ r,\ A) = \sqrt{s(s-s_0)}\, R(s) \left\{ \frac{U(s)}{(a_6^2+r^2)^2} + \frac{V(s)}{a_7^4+r^4} + \frac{W(s)}{(a_8^2-r^2)^2+a_9^4} + \frac{Z(s)}{(a_{10}^2-r^2)^2+a_{11}^4} \right\},$$

in which

$$U(s) = a_{12} R(s)^{a_{13}} + i a_{14};$$
$$V(s) = a_{15} R(s)^{a_{16}} + i a_{17};$$
$$W(s) = a_{18} R(s)^{a_{19}} + i a_{20};$$
$$Z(s) = a_{21} R(s)^{a_{22}} + i a_{23}.$$

Accordingly, in the momentum space the amplitude $T(s,t,A)$ has the form

$$T(s,\ t,\ A) = \frac{\sqrt{s(s-s_0)}}{\sinh \chi} R(s) \{ U(s)\, m(s)\, \chi \exp(-RU\chi)$$
$$+ V(s) \sin(RV\chi) \exp(-RV\chi)$$
$$+ W(s) \sin(RW_+\chi) \exp(-RW_-\chi)$$
$$+ Z(s) \sin(RZ_+\chi) \exp(-RZ_-\chi)\},$$

where

$$RU = a_6 m(s);$$
$$RV = a_7 m(s);$$
$$RW_\pm = \sqrt{\frac{1}{2}\left(\sqrt{a_8^4+a_9^4} \pm a_8^2\right)}\, m(s);$$
$$RZ_\pm = \sqrt{1/2\left(\sqrt{a_{10}^4+a_{11}^4} \pm a_{10}^2\right)}\, m(s).$$

The values of the parameters A_i $(i = 1,...,23)$ and their statistical uncertainties ΔA_i are given in Table II.[8)]

The amplitude $T(s,t,A)$ describes the experimental data on the differential and total cross sections of elastic pp scattering and the ratio $\rho(s)$ at energies $\sqrt{s} \geqslant 10$ GeV and momentum transfers in the interval $0.0375 \leqslant |t| \leqslant 9.75$ GeV^2. Figures 1–4 give graphs of the experimental data and the resulting description.

In accordance with the optical theorem and the explicit form of the amplitude, the behavior of the total cross section is determined by the function

$$\sigma_t(s) = 2\pi R^2(s). \qquad (16)$$

Therefore, (14) can be interpreted as the effective range of the

[8)]In Table II, we have omitted the dimensions of the parameters, which are obvious from the analytic expression for the amplitude and from the chosen normalization for the differential cross section.

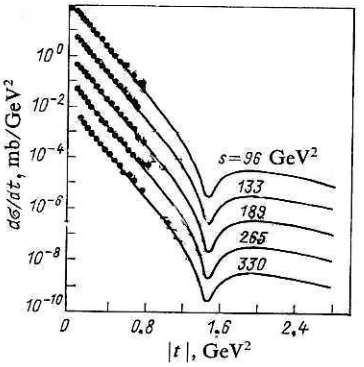

FIG. 1. Description of the experimental Fermilab data on $(d\sigma/dt)(s,t)$ at different energies. For each curve, the corresponding value of $(d\sigma/dt)(s,t)$ is divided by 10^{n-1}, where $n = 1,...,5$.

pp interaction. As can be seen from Eq. (13), the mass of the effective particle is also proportional to $R(s)$:

$$m(s) = a_1 R(s).$$

Since the dependence of the amplitude on the momentum transfer can be expressed in terms of the rapidity transfer, it is readily verified that the amplitude and, accordingly, the differential cross section satisfy the property of geometrical scaling.[32]

In Fig. 5 we give the predictions for the diffraction picture of the elastic differential cross section at all kinematically possible momenta and higher energies.

Figure 6 gives the dependence of the real and imaginary parts of the elastic pp scattering amplitude on r at the energies 100, 500, and 1000 GeV^2.

If our expression for the differential cross section is represented in the form

$$\frac{d\sigma}{dt}(s,\ t) = \frac{1}{s^N} f\left(-\frac{t}{s}\right),$$

then for $s \to \infty$ and fixed $-t/s$ we obtain

$$N = 1 + RV(s).$$

Thus, it follows from this model for the existing experimental data that:

a) the quark counting rules[33] are satisfied only for $\sqrt{s} = 10^5$–10^6 GeV;

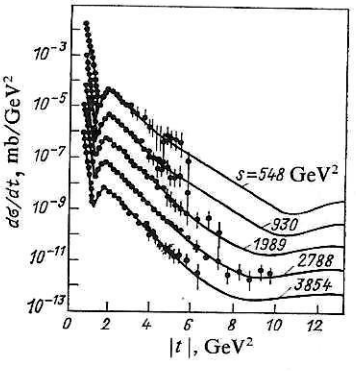

FIG. 2. Description of the experimental CERN ISR data on $(d\sigma/dt)(s,t)$ at different energies. For each curve, the corresponding value of $(d\sigma(s,t)/dt)(s,t)$ is divided by 10^{n-1}, where $n = 1,...,5$.

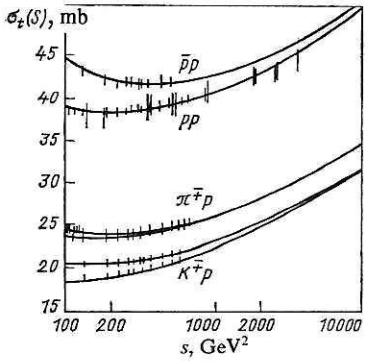

FIG. 3. Experimental data and graphs of the total cross sections $\sigma(s)$ of the $\bar{p}p$, pp, $\pi^{\mp}p$, and $K^{\mp}p$ interactions.

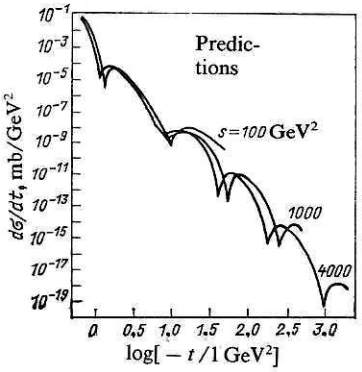

FIG. 5. Predictions for $(d\sigma/dt)(s,t)$ at different energies.

b) they hold for $\sqrt{s} \geqslant 10^5$ GeV, but the total cross sections no longer change with the energy.

For the total cross section in the limit $s \to \infty$ we obtain

$$\lim_{s\to\infty} \sigma_t(s) = c_1 + c_2 \ln^2 (s/s01),$$

which agrees with the rapid-growth model.[15]

The asymptotic behavior of $\rho(s)$ is determined by

$$\lim_{s\to\infty} \rho(s) = c\,(\ln (s/s01))^{3,5}.$$

4. DEPENDENCE OF THE EFFECTIVE RANGE OF SOME HADRON–HADRON INTERACTIONS ON THE QUANTUM NUMBERS

It is well known that the hadrons can be classified by their quantum numbers: mass m, baryon number b, electric charge q, isotopic spin I, its third projection i_3, spin J, number of constituent quarks K, etc. At present, it is not known whether these quantum numbers are independent. Moreover, in the theory of the electroweak and strong interactions they are expressed in terms of the quantum numbers of their constituent quarks.[34]

Using the dependence (16) of the total pp interaction cross section on the effective range, we assume that the parameters of $R(s)$ depend on the quantum numbers of the colliding hadrons. We describe the total cross sections for interaction of $\bar{p}$, p, $\pi^{\mp}$, $K^{\mp}$ with the proton, neutron, and deuteron at energies $\sqrt{s} \geqslant 10$ GeV by means of the expression

$$\sigma_t(s) = 2\pi R^2(s, A, \alpha),$$

where α is the set of quantum numbers, and A is an unknown set of parameters. For convenience, we rewrite the expression (14) as

$$R(s, A, \alpha) = R_1(A, \alpha) + R_2(A, \alpha)/(s/R_5(A, \alpha))^{R_3(A,\alpha)} + R_4(A, \alpha) \ln (s/R_5(A, \alpha)). \quad (17)$$

We seek the unknown functions $R_i(A,\alpha)$, $i = 1,\ldots,5$, in the form of a Taylor series up to the terms quadratic in α with unknown coefficients A for the following set of quantum numbers:

Mass $M = m_1 + m_2$.

Baryon number $B = b_1 + b_2$.

Charge $Q = q_1 + q_2$.

Isospin $I(I+1) = (I_1 + I_2)(I_1 + I_2 + 1)$.

Isospin projection $I_3 = i_{31} + i_{32}$.

Spin $J(J+1) = (J_1 + J_2)(J_1 + J_2 + 1)$.

To determine the values of the parameters and their statistical uncertainties, we solve by the method of Ref. 16 the following system of nonlinear equations:

$$\sigma_t^{\exp} = \sigma_t^{\text{theor}}(s, A, \alpha).$$

The solution leads to the following parametrization for the effective range $R(s,A,\alpha)$ and the values of $R_i(A,\alpha)$,

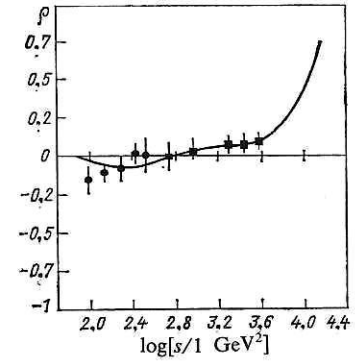

FIG. 4. Description of the experimental data for $\rho = \text{Re}\,T(s,0)/\text{Im}\,T(s,0)$: black circles, Fermilab; black squares, CERN ISR.

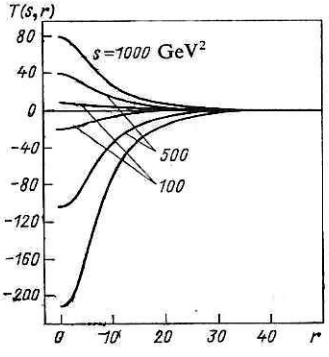

FIG. 6. Imaginary (upper curves) and real (lower curves) parts of the pp elastic-scattering amplitude as a function of r at different energies.

TABLE III. Values of the parameters A_i $(i = 1,...,21)$ of the effective range and their statistical uncertainties ΔA_i.

N	A	$\pm\Delta A$	N	A	$\pm\Delta A$
1	0.7114	0.0218	12	0.0484	0.0070
2	−0.2332	0.0168	13	−0.0708	0.0041
3	0.0223	0.0033	14	−0.0185	0.0003
4	−0.3757	0.0131	15	0.0332	0.0020
5	2.4898	0.0394	16	0.0025	0.0012
6	0.1879	0.0039	17	0.0706	0.0032
7	0.0176	0.0027	18	0.1764	0.0015
8	−0.3814	0.0086	19	0.0055	0.0002
9	0.4077	0.0222	20	−0.0050	0.0005
10	−0.2193	0.0031	21	1.8115	0.0563
11	0.3202	0.0106			

$i = 1,...,5$:

$$
\left.
\begin{aligned}
&R(s,\ A,\ \alpha) = R_1 + R_2/(s/R_5)^{R_3} + R_4 \ln(s/R_5);\\
&R_1 = A_1 M + A_2 J(J+1) + A_3 I(I+1) + A_4 \mid S \mid;\\
&R_2 = A_5 + A_6 K + A_7 \mid B \mid + A_8 \mid Q \mid + A_9 \mid I_3 \mid + A_{10} \mid Y \mid;\\
&R_3 = A_{11} + A_{12} M + A_{13} J(J+1) + A_{14} \mid Q \mid + A_{15} I(I+1)\\
&\qquad + A_{16} \mid I_3 \mid + A_{17} \mid S \mid;\\
&R_4 = A_{18} + A_{19} K + A_{20} I(I+1);\\
&R_5 = A_{21},
\end{aligned}
\right\} \tag{18}
$$

where $Y = y_1 + y_2$ is the hypercharge, $S = s_1 + s_2$ is the strangeness, and $K = k_1 + k_2$ is the number of quarks. These quantum numbers do not occur in the original set. When the system is solved, it is found that the numerical equality $A_i = -A_j$ holds in the combinations $A_i Q + A_j I_3$. Therefore, it is found from the experimental data for the total cross sections and the considered model of the effective range of the hadron–hadron interactions that the quantum numbers Q and I_3 contribute to the parameters of the effective range through the hypercharge quantum number: $Y = 2(Q - I_3)$. The dependence of the parameters on the strangeness quantum number $S = Y - B$ is obtained similarly.

In Table III, we give the values of the parameters A_i $(i = 1,...,21)$ and their statistical uncertainties.[9)]

The value of the scale parameter $s01$ used in (14) is equal to the parameter $R_5 = A_{21}$ determined here, which is the same for all processes (i.e., does not depend on the quantum numbers), and $\chi^2/(M - N) = 1.11$.

In Figs. 3, 7, and 8 we compare the theoretical descriptions with the experimental data.

It is readily verified that the effective range of the hadron–hadron interactions as a function of the quantum numbers of the colliding hadrons is CPT-invariant:

$$\sigma_t(a,\ b) = \sigma_t(\bar{a},\ \bar{b}).$$

Our description is consistent with the theorems of Froissart[35,36] and Pomeranchuk.[37] And since there is a good description of the expermental data, it can be asserted on this basis that the contemporary experimental data indicate the validity of these theorems.

[9)]For the dimensions of the parameters A_i $(i = 1,...,21)$, see the expression for the effective range.

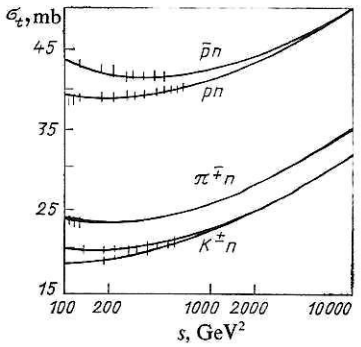

FIG. 7. Experimental data and graphs of the total cross sections $\sigma_{tot}(s)$ of $\bar{p}n$, pn, $\pi^{\mp}n$, and $K^{\mp}n$ interactions.

The calculated effective range $R(s)$ makes it possible for given quantum numbers of the colliding hadrons to predict the behavior of the total cross sections at high energies, for example,

a) the total cross sections for the interactions of the strange particles Λ, $\Sigma^{\pm}$, Ξ^{-} with the proton (Fig. 9);

b) the $\pi^+\pi^+$ total cross section (Fig. 9);

c) the total cross sections for scattering of the proton on the light nuclei T, ^{3}He, ^{4}He (Fig. 10).

The quantum numbers of the light nuclei are obtained additively from the quantum numbers of the protons and neutrons that constitute them.

Our predictions for the hyperon–proton total cross sections and for the p^4He total cross section agree with the preliminary experimental data of Ref. 38. We note that these predictions have an approximately 10% error corridor, which is due to the inadequacy of the experimental data for the antiproton and pion total cross sections at the higher energies. Since we have a good description of the experimental data in terms of the effective range, we can check the quark sum rules at different energies. In Fig. 11 we show the ratios of the right-hand sides to the left-hand sides as functions of the energy for the quark sum rules obtained in Refs. 5 and 39:

1) $6\sigma_{\pi N} = 3\sigma_{KN} + 2\sigma_{NN}$;
2) $6\sigma_{\pi^- p} = 3\sigma_{K^+ p} = 2\sigma_{pn} + 6\sigma_{K^- p}$;
3) $6\sigma_{pp} + \sigma_{\Sigma^- p} = \sigma_{\Lambda p} + 6\sigma_{pn}$;
4) $4\sigma_{\pi^+ p} = 2\sigma_{\pi^- p} + 7/8\sigma_{K^+ p} + 3/4\sigma_{pp}$.

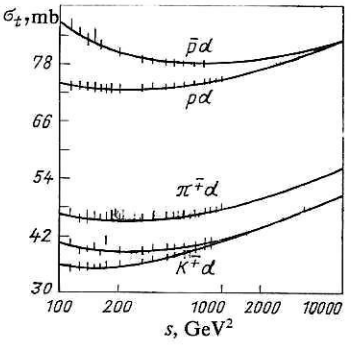

FIG. 8. Experimental data and graphs of the total cross sections $\sigma_{tot}(s)$ of $\bar{p}d$, pd, $\pi^{\mp}d$, and $K^{\mp}d$ interactions.

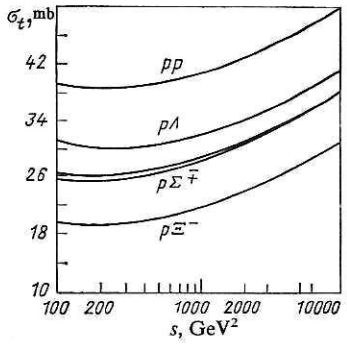

FIG. 9. Predictions for the total cross sections $\sigma(s)$ of pp, $p\Lambda$, $p\Sigma^{\mp}$, and $p\Xi^{-}$ interactions.

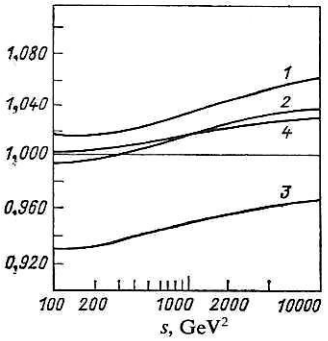

FIG. 11. Behavior of the quark sum rules (1–4) with increasing energy.

The data on the total cross sections obtained in cosmic-ray experiments[40] confirm the predictions of our description.

5. EFFECTIVE RANGE AND TOTAL CROSS SECTIONS OF HADRON–HADRON INTERACTIONS FROM THE THRESHOLD ENERGIES

In this section, we test whether the total hadron–hadron cross sections can be described from the threshold energies by means of the expression (16). We assume that the effective range can be represented as a sum of a definite number of Breit–Wigner functions and a logarithmic term:

$$R(s)=\sum_i \frac{\rho_i^2(s)}{(\sqrt{s}-\mu_i)^2+\Gamma_i^2(s)}+R(\ln(s/s_0))^A. \qquad (19)$$

Because of the huge amount of experimental material, numerical analysis of the correlation dependences between the parameters $\rho_i, \mu_i, \Gamma_i, A$ makes it possible to determine with high accuracy the uncertainty in the exponent of the logarithmic term.

We determine the unknown functions ρ_i and Γ_i, the values of the unknown parameters, their statistical uncertainty, and the number of Breit–Wigner functions by using the method of Ref. 16 to solve the system $\sigma_t^{\exp}(s)=2\pi R^2(s)$, where $\sigma_t(s)$ are the values of the total interaction cross sections of $\bar{p}, p, \pi^{\mp}, K^{\mp}$ with the proton. The number of experimental points for these processes are, respectively, 143, 131, 500, 326, 254, 144. The solution of the overdetermined system showed that $\rho_i^2(s)=s\rho_i^2$, $\Gamma_i^2(s)=s\Gamma_i^2$, and the number of structures is $n=7$.

Tables IV–VI give the values obtained for the parameters and their statistical uncertainties. The quantity R_0 has the form

$$R_0=\sum_{i=1}^{7}\frac{\rho_i^2}{1+\Gamma_i^2},$$

where ρ_i and Γ_i are the values of the parameters of the corresponding process. The asterisk identifies parameters common to one isotopic multiplet.

Figures 12–17 show the experimental data and the theoretical description, and also the effective range and its structure. It can be seen that our solution gives a good description of the experimental data. The values of

$$\chi^2=\frac{1}{M-N}\sum_i^M\left(\frac{\sigma_t^{\exp}(s_i)-\sigma_t^{\text{theor}}(s_i)}{\Delta_i}\right)^2$$

for nucleons, pions, and kaons are, respectively, 1.133, 1.010, and 1.060, where Δ_i are the experimentally observed statistical errors.

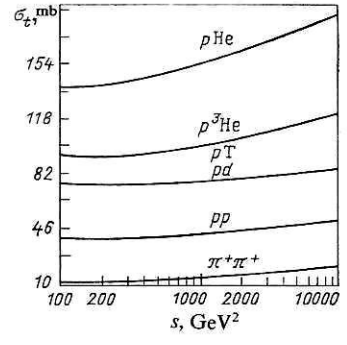

FIG. 10. Predictions for the total cross sections $\sigma(s)$ of the proton on T, ^{3}He, He, and π^+ on π^+.

TABLE IV. Values of the parameters of the effective interaction range (19) for $\bar{p}p$ and pp interactions.

ρ	$\Delta\rho$	μ	$\Delta\mu$	Γ	$\Delta\Gamma$
$\bar{p}p$ ($R_0=0,906\pm0.353$)					
0,0259	±0,0123	1,8929	±0,0081	0,0196	±0,0047
0,1917	±0,0857	1,9198	±0,0432	0,1115	±0,0303
0,2704	±0,1171	2,2672	±0,0309	0,1984	±0,0415
0,2703	±0,1150	2,7916	±0,0296	0,2431	±0,0483
0,3464	±0,1041	3,8160	±0,0764	0,3262	±0,0536
0,6315	±0,1114	6,4937	±0,1362 *	0,6157	±0,0643 *
0,8842	±0,0882	15,0292	±0,3446 *	1,1628	±0,0312 *
pp ($R_0=0,856\pm0,392$)					
0,0222	±0,0043	1,9691	±0,0020	0,0282	±0,0040
0,0419	±0,0100	2,2055	±0,0041	0,0586	±0,0078
0,2580	±0,0551	2,3606	±0,0361	0,2104	±0,0226
0,2716	±0,2022	2,9249	±0,0619	0,3051	±0,1056
0,4427	±0,2098	3,9992	±0,1514	0,4555	±0,0980
0,5234	±0,1296	6,4937	±0,1362 *	0,6157	±0,0643 *
0,9221	±0,0637	15,0292	±0,3446 *	1,1628	±0,0312 *

* $R=0,2428\pm0,0023$; $A=0,9993\pm0,0030$.

TABLE V. Values of the parameters of the effective interaction range (19) for $\pi^- p$ and $\pi^+ p$ interactions.

ρ	$\Delta\rho$	μ	$\Delta\mu$	Γ	$\Delta\Gamma$
$\pi^- p$ ($R_0 = 0.696 \pm 0.087$)					
0.1073	±0.0006	1.2204	±0.0003	0.0651	±0.003
0.1188	±0.0012	1.4981	±0.0004	0.0952	±0.0008
0.0351	±0.0005	1.6800	±0.0003	0.0332	±0.0003
0.0641	±0.0028	1.8430	±0.0008	0.0879	±0.0022
0.2560	±0.0166	2.1819	±0.0039	0.2423	±0.0087
0.5992	±0.0525	3.3347	±0.0212 *	0.5831	±0.0326 *
0.9055	±0.0710	8.3813	±0.1397 *	1.2014	±0.0406 *
$\pi^+ p$ ($R_0 = 0.672 \pm 0.082$)					
0.1073	±0.0010	1.2233	±0.0003	0.0494	±0.0003
0.1014	±0.0024	1.3233	±0.0021	0.0862	±0.0013
0.0676	±0.0017	1.6700	±0.0007	0.0831	±0.0014
0.0906	±0.0008	1.8993	±0.0004	0.0849	±0.0005
0.1958	±0.0122	2.3490	±0.0020	0.2185	±0.0064
0.5863	±0.0508	3.3347	±0.0212 *	0.5831	±0.0326 *
0.9176	±0.0709	8.3813	±0.1397 *	1.2014	±0.0406 *

* $R = 0.1814 \pm 0.0024$; $A = 0.9996 \pm 0.0043$.

On the basis of our description of the experimental data and the explicit form of the effective range, we can interpret its structure as follows:

a) the Breit–Wigner components correspond to the contributions of the different interaction channels with subsequent increase in the number of produced particles by the production of particle–antiparticle pairs;

b) the Froissart term corresponds to the transition to a statistical nature of multiparticle production at energies above 10–20 GeV.

The exponent A of the logarithmic term is determined with high accuracy. For the proton–proton total cross section $A = 0.999 \pm 0.003$, while for the remaining processes $A = 0.999 \pm 0.004$.

In the limit $s \to \infty$, the asymptotic behavior of the effective range has the form

$$R(s) = R_0 + R \ln (s/s_0).$$

From comparison of our description for the total cross sections at very high energies with their asymptotic behavior as $s \to \infty$ we can estimate the Froissart energy (i.e., the energy above which Froissart's theorem holds[35,36]). In Fig. 18 we compare the behavior of the total cross sections (continuous curves) with their asymptotic expression up to $\sqrt{s} = 10^3$ GeV (broken curves). It can be seen that for all processes the asymptotic behavior commences (with 10% error) at the same energy—the Froissart energy. The value of this energy lies in the interval 10^5–10^6 GeV or 300–1000 GeV, or 10^{-16}–10^{-17} cm^{-1}.

Figure 19 shows the lower error corridor for the total reaction cross sections of $\bar{p}$, π^-, and K^- with the proton (continuous curves) and the upper error corridor for the total cross sections of p, π^+, and K^+ with the proton (broken curves). It can be seen that our description confirms Pomeranchuk's theorem.[37] The contemporary experimental data and our description are such that one can predict the value of the Pomeranchuk energy (the energy from which the theorem of Ref. 37 holds) for $\bar{p}, p, \pi^\mp$, and $K^\mp$ interactions with the proton; this energy is, respectively, of the order 10^5, 2×10^2, 10^3 GeV^2.

The consistency of our description with the experimental data can be seen from the fact that for $\pi^\mp$ scattering on the proton the predicted value of the Pomeranchuk energy agrees with the energy already observed (see Figs. 14 and 15,

TABLE VI. Values of the parameters of the effective interaction range (19) for $K^- p$ and $K^+ p$ interactions.

ρ	$\Delta\rho$	μ	$\Delta\mu$	Γ	$\Delta\Gamma$
$K^- p$ ($R_0 = 0.600 \pm 0.140$)					
0.1038	±0.0031	1.4836	±0.0015	0.0619	±0.0015
0.0411	±0.0024	1.6985	±0.0010	0.0528	±0.0022
0.0419	±0.0014	1.8146	±0.0006	0.0431	±0.0010
0.0324	±0.0011	2.0640	±0.0006	0.0573	±0.0011
0.5421	±0.0281	2.3310	±0.0092	0.4331	±0.0158
0.5663	±0.1093	4.9226	±0.01100 *	0.7006	±0.0943 *
0.5412	±0.1468	11.4578	±0.3851 *	1.1793	±0.1192 *
$K^+ p$ ($R_0 = 0.533 \pm 0.167$)					
0.0983	±0.0051	1.5208	±0.0014	0.0978	±0.0044
0.1000	±0.0103	1.8532	±0.0035	0.1210	±0.0066
0.1435	±0.0298	2.1694	±0.0126	0.1930	±0.0207
0		2.3738	±1.8847	0.2305	±0.8315
0.3865	±0.0659	2.9879	±0.0428	0.4322	±0.0497
0.4933	±0.1109	4.9226	±0.1100 *	0.7006	±0.0943 *
0.7000	±0.1418	11.4578	±0.3851 *	1.1793	±0.1192 *

* $R = 0.1941 \pm 0.0052$; $A = 0.9998 \pm 0.0036$.

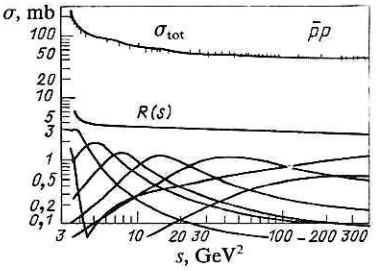

FIG. 12. Experimental data and graph of the total cross section $\sigma(s)$ for $\bar{p}p$ interactions (upper curve); graph of the effective range $R(s) = \Sigma_{i=1}^{n} s\rho_i^2/(\sqrt{s}\,\mu_i)^2 + s\Gamma_i^2 + R \ln(s/s_0)^4$ of the interaction and its structure (lower curves).

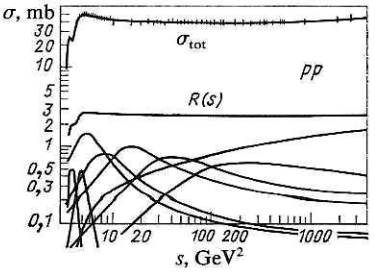

FIG. 13. The same as in Fig. 12 for pp interactions.

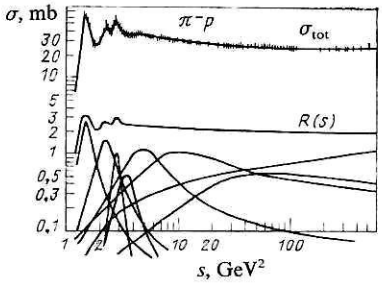

FIG. 14. The same as in Fig. 12 for $\pi^- p$ interactions.

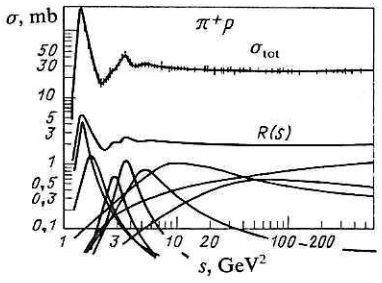

FIG. 15. The same as in Fig. 12 for $\pi^+ p$ interactions.

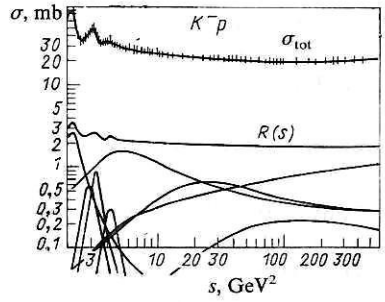

FIG. 16. The same as in Fig. 12 for $K^- p$ interactions.

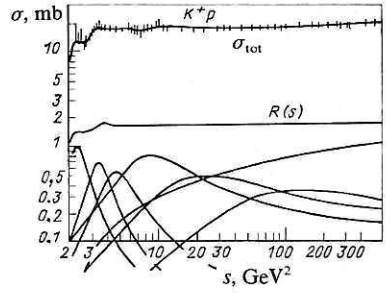

FIG. 17. The same as in Fig. 12 for $K^+ p$ interactions.

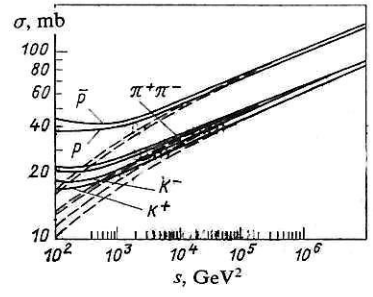

FIG. 18. Total cross sections of hadron interactions (continuous curves) and their asymptotic behavior (broken curves).

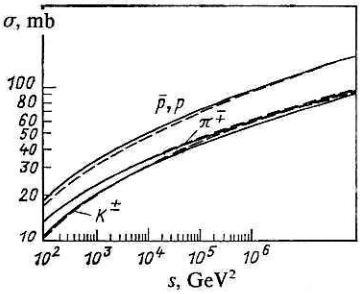

FIG. 19. Lower error corridor for the total cross sections of $\bar{p}p$, $\pi^- p$, $K^- p$ interactions (continuous curves) and upper error corridor for the cross sections of pp, $\pi^+ p$, $K^+ p$ interactions (broken curves).

which show that the experimental error corridors of the two processes after 200 GeV^2 have a nonempty intersection).

Equality of the coefficients of the logarithmic term for particles belonging to the same isotopic multiplet is consistent with the three-quark hadron model.[41]

6. BASIC RESULTS AND PREDICTIONS

On the basis of simple quantum-mechanical ideas, representing the pp elastic-scattering amplitude in the space of the relativistic relative coordinate, we have constructed the elastic-scattering amplitude in a scalar approximation, describing $(d\sigma/dt)(s,t)$ and $\sigma_t(s)$ for $\sqrt{s} \geqslant 10$ GeV and $0.0375 \leqslant |t| \leqslant 9.75$ GeV^2. We have confirmed the properties of geometrical scaling and the quark counting rules. The amplitude depends on the energy through the function

$$R(s) = R_0 + R_1/(s/s01)^{\alpha} + R \ln (s/s01),$$

which in accordance with the optical theorem and the explicit form of the amplitude determines the total cross section by the relation

$$\sigma_t(s) = 2\pi R^2(s).$$

The function $R(s)$ is interpreted as the effective range of the hadron–hadron interaction. As $s \to \infty$, our description confirms the model of maximal growth of the total cross sections. The mass of the effective particle is proportional to $R(s)$.

On the basis of the experimental data on the interaction of $\bar{p}, p, \pi^{\mp}, K^{\mp}$ with the proton, neutron, and deuteron in terms of the effective range, we have obtained the dependence of the hadron–hadron cross sections at energies $\sqrt{s} \geqslant 10$ GeV on the quantum numbers of the colliding hadrons. We have analyzed the validity of some quark counting rules with increasing energy. We have obtained a description of the total cross sections of $\bar{p}p$, pp, $\pi^{\mp} p$, $K^{\mp} p$ interactions from the threshold energies in the form

$$\sigma_t(s) = 2\pi R^2(s),$$

where

$$R(s) = \sum_{i=1}^{7} \frac{s\rho_i^2}{(\sqrt{s}-\mu_i)^2 + s\Gamma_i^2} + R(\ln s/s_0)^A, \quad (A = 0.999 \pm 0.004).$$

The high-energy asymptotic behavior of this expression for the pp total interaction cross sections agrees with the asymptotic behavior of the function that determines the de-

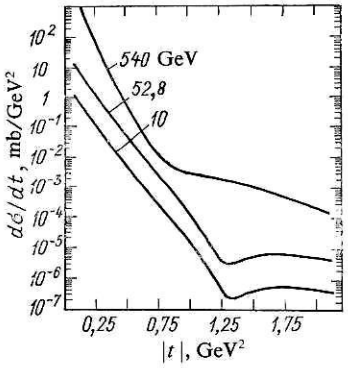

FIG. 20. Predictions for $(d\sigma/dt)(s,t)$ at different energies $\sqrt{s}$ and $0.25 \leqslant |t| \leqslant 1.75$ GeV^2 for elastic $\bar{p}p$ scattering. The values of $(d\sigma/dt)(s,t)$ for each curve are multiplied by 10^{n-1}, where $n = 1, 3, 5$.

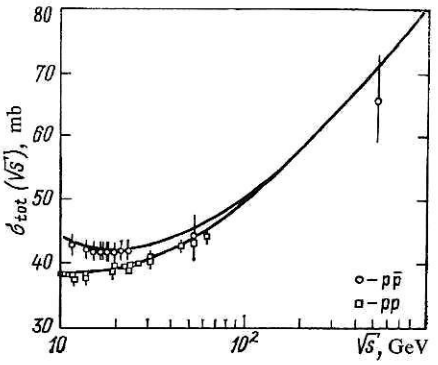

FIG. 22 Predictions for the total cross sections of $\bar{p}p$ and pp interactions for $10 \leqslant \sqrt{s} \leqslant 10^3$ GeV. It can be seen that they agree with the total cross section of pp scattering at $\sqrt{s} = 540$ GeV measured with the SPS Collider.

pendence of the elastic hadron–hadron amplitude on the energy. The form obtained for the effective range makes it possible to formulate conditions for the onset of asymptotic behavior in the sense of Froissart's theorem. The resulting behavior agrees with Pomeranchuk's theorem.

On the basis of the resulting elastic pp interaction amplitude we have predicted the diffraction picture of the elastic differential cross sections.

The dependence found for the effective range on the quantum numbers for $\sqrt{s} \geqslant 10$ GeV makes it possible to predict the behavior of the total hyperon–proton cross section and the cross sections for proton interactions on light nuclei. If the resulting dependence of the effective range on the quantum numbers is used, the behavior of the other hadron–hadron elastic differential cross sections can be predicted.[42]

Figure 20 gives the predictions for $(d\sigma/dt)(s,t)$ for elastic $\bar{p}p$ scattering. Figure 21 gives the experimental data and graphs for $(d\sigma/dt)(s,t)$ at $\sqrt{s} = 10$ and 52.8 GeV and for $0.25 \leqslant |t| \leqslant 1.75$ GeV^2. On the upper curve we give the prediction of the behavior at $\sqrt{s} = 540$ GeV for elastic pp scattering. Figure 22 gives the behavior of the total cross sections for $\bar{p}p$ and pp interactions for $10 \leqslant \sqrt{s} \leqslant 10^3$ GeV. The value of the $\bar{p}p$ total interaction cross section at $\sqrt{s} = 540$ GeV calculated by means of the expressions (16)–(18) is $\sigma_{tot}^{theor}(\sqrt{s} = 540$ GeV$) = 71 \pm 4$ mb. The corresponding experimental value is[43]

$$\sigma_{tot}^{exp} \ (\sqrt{s} = 540\,\text{GeV}) = (66 \pm 7)\,\text{mb}.$$

We hope that in the coming years data will become available on proton–meson elastic scattering at energies $\sqrt{s} > 10$ GeV and squared momentum transfer $|t| \geqslant 10$ GeV^2, which will make it possible to find the dependence of the effective mass on the masses of the colliding particles, and also to verify the predicted diffraction picture of elastic pp scattering.

We should like to express our thanks for numerous discussions, helpful advice, and critical comments to our colleagues at the Laboratory of Theoretical Physics of the Joint Institute for Nuclear Research and at the theory departments of the Institute of High Energy Physics and the Institute of Nuclear Research of the USSR Academy of Sciences.

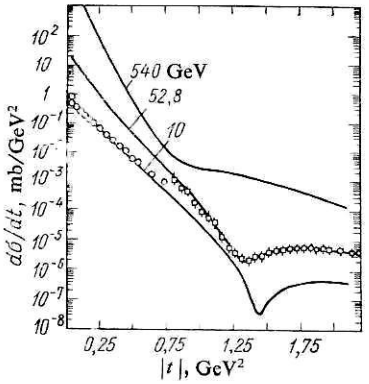

FIG. 21. Experimental data and graphs for $(d\sigma/dt)(s,t)$ at different energies $\sqrt{s}$ and $0.25 \leqslant |t| \leqslant 1.75$ GeV^2 for elastic pp scattering. The prediction for $(d\sigma/dt)(s,t)$ at $\sqrt{s} = 540$ GeV. The values of $(d\sigma/dt)(s,t)$ for each curve are multiplied by 10^{1-n}, where $n = 1, 2, 3$.

[1]N. N. Bogolyubov, in: Fizika vysokikh énergiĭ i teoriya élementarnykh chastits (High Energy Physics and the Theory of Elementary Particles), Naukova Dumka, Kiev (1967), p. 5.
[2]A. A. Logunov and A. N. Tavkhelidze, Nuovo Cimento **29**, 380 (1963).
[3]V. G. Kadyshevsky, Nucl. Phys. **B86**, 125 (1968); V. G. Kadyshevsky and M. D. Matveev, Nuovo Cimento **A55**, 276 (1967); V. G. Kadyshevskiĭ, R. M. Mir-Kasimov, and N. B. Skachkov, Fiz. Elem. Chastits At. Yadra **2**, 635 (1972) [Sov. J. Part. Nucl. **2**, Part 3, 69 (1972)].
[4]N. B. Skachkov and I. L. Solovtsov, Fiz Elem. Chastits At. Yadra **9**, 5 (1978) [Sov. J. Part. Nucl. **9**, 1 (1978)]; I. V. Amirkhanov, G. V. Grusha, and R. M. Mir-Kasimov, Fiz. Elem. Chastits At. Yadra **12**, 651 (1981) [Sov. J. Part. Nucl. **12**, 262 (1981)].
[5]S. P. Denisov *et al.*, Nucl. Phys. **B65**, 1 (1973).
[6]E. Bracci *et al.*, Preprint CERN HERA 72-1.2 (1972), 73-1 (1973); V. Egert *et al.*, Nucl. Phys. **B98**, 93 (1975); E. Nagy *et al.*, Nucl. Phys. **B150**, 221 (1979).
[7]D. S. Ayres *et al.*, Phys. Rev. D **15**, 3105 (1977); A. S. Carrol *et al.*, Phys. Lett. **B80**, 423 (1979).
[8]A. Bohm *et al.*, Phys. Lett. **B49**, 491 (1974).
[9]L. A. Fajardo *et al.*, Preprint Fermilab 80-27 (1980).
[10]T. T. Wu and C. N. Yang, Phys. Rev. **137**, B708 (1965); T. T. Chou and C. N. Yang, Phys. Lett. **20**, 1213 (1968); Phys. Rev. **170**, 1521 (1968); **175**, 1832 (1968); V. Amaldi, M. Jacob, and G. Matthial, Ann. Rev. Nucl. Sci. **26**, 385 (1976).
[11]V. T. Garsevanishvili, V. A. Matveev, and L. A. Slepchenko, Fiz. Elem. Chastits At. Yadra **1**, 91 (1970) [Sov. J. Part. Nucl. **1**, Part 1, 52 (1970)]; M. I. Dzhgarkava *et al.*, Nucl. Phys. **B79**, 396 (1974).
[12]R. J. Glauber, in: Lectures in Theoretical Physics, Vol. 1, Interscience, London (1959), p. 315; V. R. Garsevanishvili *et al.*, Teor. Mat. Fiz. **6**, 36 (1971); B. M. Barbashov *et al.*, Fiz. Elem. Chastits At. Yadra **4**, 623 (1973) [Sov. J. Part. Nucl. **4**, 261 (1973)]; S. V. Goloskokov, S. P. Kule-

shov, and O. V. Selyugin, Yad. Fiz. **31**, 741 (1980) [Sov. J. Nucl. Phys. **31**, 385 (1980)].
[13]V. P. Gerdt, V. I. Inozemtsev, and V. A. Meshcheryakov, Yad. Fiz. **24**, 176 (1976) [Sov. J. Nucl. Phys **24**, 90 (1976)]; V. P. Gerdt and V. A. Meshcheryakov, Preprint R2-9572 [in Russian], JINR, Dubna (1976).
[14]I. Van Hove and K. Fialkovski, Nucl. Phys. **B107**, 211 (1976); L. Van Hove, Nucl. Phys. **B122**, 525 (1977); S. Wakaizumi and W. Tanimoto, Phys. Lett. **B70**, 55 (1977); A. Bialas *et al.*, Acta Phys. Pol. **B8**, 855 (1977); E. M. Levin *et al.*, Preprint No. 444, Leningrad Institute of Nuclear Physics (1978).
[15]L. D. Solov'ev and A. V. Shchelkachev, Fiz. Elem. Chastits At. Yadra **6**, 571 (1975) [Sov. J Part. Nucl. **6**, 229 (1975)].
[16]L. Aleksandrov, Zh. Vychisl. Mat. Mat. Fiz. **11**, 36 (1971); Preprint R5-5511 [in Russian], JINR, Dubna (1970); Preprint B1-59966 [in Russian], JINR, Dubna (1976).
[17]R. Hagedorn and J. Reinfelds, "Sigma without effort," CERN 78-08, Geneva (1978).
[18]R. Brun and H. Watkins, HPLOT, DD/EE/80-2, CERN, Geneva (1980).
[19]H. Bethe and E. Salpeter, Phys. Rev. **84**, 1232 (1951).
[20]V. G. Kadyshevskiĭ and A. N. Tavkhelidze, in: Problemy teoretcheskoĭ fiziki (Problems of Theoretical Physics), Nauka, Mscow (1969), p. 261; A. A. Logunov and A. A. Khrustalev, in: Problemy teoreticheskoĭ fiziki (Problems of Theoretical Physics), Nauka, Moscow (1972), p. 96; I. Todorov and V. Risov, Zadachata za dvete tela v kvantovata teoriya (The Two-Body Problem in Quantum Theory) [in Bulgarian], Nauka i Izkustvo, Sofia (1974); V. I. Savrin, N. E. Tyurin, and O. A. Khrustalev, Fiz. Elem. Chastits At. Yadra **7**, 21 (1976) [Sov. J. Part. Nucl. **7**, 9 (1976)]; A. N. Kvinikhidze, A. N. Sisakyan, L. A. Slepchenko, and A. N. Tavkhelidze, Fiz. Elem. Chastits At. Yadra **8**, 478 (1977) [Sov. J. Part. Nucl. **8**, 196 (1977)]; V. G. Kadyshevskiĭ, M. D. Mateev, and R. M. Mir-Kasimov, Yad. Fiz. **11**, 692 (1970) [Sov. J. Nucl. Phys. **11**, 388 (1970)]; A. D. Sonkov, V. G. Kadyshevskiĭ, M. D. Mateev, and R. M. Mir-Kasimov, in: Nelokal'nye nelineĭnye i perenormiruemye teorii polya (Nonlocal, Nonlinear, and Renormalizable Field Theories), D-2-9788, JINR, Dubna (1976), p. 36; M. D. Mateev, in: X Mezhdunarodnaya shkola molodykh uchenykh po fizike vysokikh énergiĭ (Tenth Intern. School on High Energy Physics for Young Scientists), D2-10533, JINR, Dubna (1977); A. D. Donkov, V. G. Kadyshevskiĭ, and M. D. Mateev, Preprint R2-80-568 [in Russian], JINR, Dubna (1980).
[21]L. D. Landau and E. M. Lifshitz, Kvantovaya mekhanika, Nauka, Moscow (1974); English translation: Quantum Mechanics, Pergamon Press, Oxford (1974).
[22]I. M. Lévy-Leblond, Galilei Group: Galilean Invariance in Group Theory and its Applications (ed. E. Loebel), New York (1971).
[23]M. A. Naĭmark, Lineĭnye predstavleniya gruppy Lorentsa, Nauka, Moscow (1958); English translation: Linear Representations of the Lorentz Group, Pergamon Press, London (1964).
[24]S. Cht. Mavrodiev, Preprint E2-7910 [in English], JINR, Dubna (1974); S. Shch. Mavrodiev, Preprint 2-8487 [in Russian], JINR, Dubna (1974); S. Cht. Mavrodiev, Fizika **9**, 117 (1977).
[25]I. S. Shapiro, Dokl. Akad. Nauk SSSR **106**, 647 (1956) [Sov. Phys. Dokl. **1**, 91 (1956)]; L. G. Zastavenko and Chao Kai-Hua, Zh. Eksp. Teor. Fiz. **35**, 1475 (1958) [Sov. Phys. JETP **8**, 1031 (1959)]; V. S. Popov, Zh. Eksp. Teor. Fiz. **37**, 1116 (1959) [Sov. Phys. JETP **10**, 794 (1960)].
[26]N. A. Chernikov, Fiz. Elem. Chastits At. Yadra **4**, 773 (1973) [Sov. J. Part. Nucl. **4**, 315 (1973)]; N. A. Chernikov and N. S. Shavokhina, Teor. Mat. Fiz. **42**, 59 (1980); **43**, 359 (1980).
[27]I. T. Todorov, Phys. Rev. D **3**, 2351 (1971).
[28]S. Shch. Mavrodiev, Preprint R2-8897 [in Russian], JINR, Dubna (1975); L. Alexandrov and S. Cht. Mavrodiev, Preprint E2-9936 [in English], JINR, Dubna (1976); S. B. Drenska and S. Shch. Mavrodiev, Yad. Fiz. **28**, 749 (1978) [Sov. J. Nucl. Phys. **28**, 385 (1978); L. Aleksandrov, S. B. Drenska, and S. Shch. Mavrodiev, Yad. Fiz. **32**, 520 (1980) [Sov. J. Nucl. Phys. **32**, 267 (1980)].
[29]N. N. Bogolyubov, A. A. Logunov, and I. T. Todorov, Osnovy aksiomaticheskogo podkhoda v kvantovoĭ polya, Nauka, Leningrad (1969); English translation: Introduction to Axiomatic Quantum Field Theory, Benjamin, New York (1975).
[30]A. T. Filippov, Preprint E2-7929 [in English], JINR, Dubna (1974).
[31]S. B. Drenska and S. Shch. Mavrodiev, B3-11-81-145, JINR, Dubna (1981).
[32]A. J. Buras and Y. Dias de Deus, Nucl. Phys. **B71**, 481 (1974); V. Barger, Plenary Session Talk at the 17th Intern. Conf. on High Energy Physics, London (1974); V. Barger, J. Luthe, and N. R. Phylips, Nucl. Phys. **B88**, 237 (1975).
[33]V. A. Matveev, R. M. Muradyan, and A. N. Tavkhelidze, Lett. Nuovo Cimento **7**, 719 (1973); S. J. Brodsky and G. Farrar, Phys. Rev. **31**, 1153 (1973).
[34]S. L. Glashow, Sci. Am. **233**, No. 4, 38 (1974); S. Weinberg, Rev. Mod. Phys. **52**, 515 (1980); M. Jacob and P. Landshoff, Sci. Am. **242**, 46 (1980).
[35]M. Froissart, Phys. Rev. **123**, 1053 (1961).
[36]A. Martin, in: Obshchie printsipy kvantovoĭ teorii polya (General Principles of Quantum Field Theory; Russian translations edited by V. A. Meshcheryakov), Nauka, Moscow (1977), p. 13; A. A. Logunov, M. A. Mestvirishvili, and V. A. Petrov, *ibid.*, p. 183.
[37]I. Ya Pomeranchuk, Zh. Eksp. Teor. Fiz. **34**, 725 (1958) [Sov Phys. JETP **7**, 499 (1958)].
[38]J. Lach and C. Pondrom, Ann. Rev. Nucl. Part. Sci. **29**, 112 (1979); Y. P. Burg *et al.*, in: Proc. of the 20th Intern. Conf. on High Energy Physics, Madison, USA, July (1980); CERN-EP-80-114 (1980).
[39]H. J. Lipkin, Nucl. Phys. **B79**, 381 (1974); R. Kang and B. Nicolescu, Phys. Rev. D **11**, 2461 (1975).
[40]G. B. Yodh, Prospects for Strong Interaction Physics at ISABELLE, BLN 50701 (1977), p. 48.
[41]P N. Bogolubov, in: Proc. of the 18th Intern. Conf. on High Energy Physics, Tbilisi; D1,2-10400, JINR, dubna (1977), p. 99.
[42]S. B. Drenska, S. Shch. Mavrodiev, A. N. Sisakyan, and G. T. Torosyan, Preprint D2-82-280 [in Russian], JINR, Dubna (1982).
[43]B. Koene *et al.*, in Physics in Collisions: High-Energy *ee*, *ep*, *pp* Interactions, Vol. 2 (eds. P. Carlson and P. Trower) (1982), p. 85; R. Battiston *et al.*, Phys. Lett. **B117**, 126 (1982).

Translated by Julian B. Barbour